Astron. Astrophys. 325, 109–123 (1997)

ASTRONOMY AND ASTROPHYSICS

Are high polarization quasars and BL Lacertae objects really different? A study of the optical spectral properties⋆

Riccardo Scarpa[1] **and Renato Falomo**[2]

[1] Space Telescope Science Institute, 3700 San Martin Drive, Baltimore, MD 21218, USA (scarpa@stsci.edu)
[2] Osservatorio Astronomico di Padova, v. Osservatorio 5, I-35122 Padova, Italy (falomo@astrpd.pd.astro.it)

Received 2 January 1997 / Accepted 20 March 1997

Abstract. The continuum and emission lines properties of a sample of 73 blazars is studied, investigating differences and similarities among normal low–polarization quasars (LPQ), radio–loud high polarized quasars (HPQ), and BL Lacertae objects (BLL).

We found that at variance with LPQ, most HPQ have power law optical continua ($f_\nu \propto \nu^\alpha$) with no indication of blue bumps or strong FeII and Balmer emission. Comparison of LPQ with blazars, considered as a class including both HPQ and BLL, confirms and put on firm statistical bases that the optical continuum of blazars ($\alpha_O = -1.00 \pm 0.09$) is significantly steeper than that of LPQ ($\alpha_O \sim -0.5$). On the other hand the average spectral index for the HPQ and BLL subsamples is rather similar ($< \alpha_{HPQ} >= -1.01 \pm 0.17$ and $< \alpha_{BLL} >= -0.99 \pm 0.11$). In the $\alpha_O - \alpha_{RX}$ plane HPQ do not split in two distinct groups as do BLL, which spilt in Radio (RBL) and X-ray selected (XBL) objects. All HPQ cluster together in the same region occupied by RBL, while XBL are clearly distinguished.

A significant correlation is found between the maximum percentage of optical polarization and both α_O and α_{RX}, the less polarized object having the steeper spectral index.

The comparison of emission line luminosities shows that LPQ have on average stronger lines ($\sim$ a factor of 6) with respect to blazars. Comparing HPQ and RBL we show they exhibit similar range of line luminosity, BL Lacs being just the objects with lines of smaller equivalent width as directly induced by the e.w.$<$5Å definition criteria.

This leads us to conclude that from the point of view of optical spectral properties HPQ and RBL are quite similar objects while XBL may be different.

Key words: BL Lacertae objects – quasars: general techniques: polarimetric – line: formation

Send offprint requests to: Riccardo Scarpa

⋆ Based on observations collected at the European Southern Observatory, La Silla, Chile.

1. Introduction

Blazars are active galactic nuclei characterized by compact luminous radio cores, high and variable radio and optical polarization ($> 3\%$), superluminal velocity, strong X-ray and γ ray emission. The continuum emission is largely, rapidly variable at all frequencies with amplitude and rapidity increasing with frequency (see e.g. reviews by Urry & Padovani 1995 and Kollgaard 1994). The overall energy distribution extends smoothly from radio to X–ray frequencies without indication of strong breaks (e.g. Impey & Neugebauer 1988, Landau et al. 1986). This emission is describable over large intervals of frequency by a simple power law model ($F_\nu \propto \nu^\alpha$, with α spectral index, e.g. Pian et al. 1994). Recently blazars have also been detected in the γ–ray domain and, indeed, many emit most of energy in the MeV-GeV band (von Montigny et al. 1995; Impey 1996). These extreme properties are usually explained in terms of relativistic beaming of the emission arising, by synchrotron self–Compton processes, in a jet closely aligned to the line of sight (Blandford & Rees 1978).

Inside the blazars family some distinction is done depending on variability, polarization and spectral line characteristics. BL Lac objects (BLL) are characterized by the lack (or weakness !) of emission lines in the optical spectrum. On the other hand, highly polarized quasars (HPQ) show strong emission lines as generally observed in low–polarization quasars (LPQ). The HPQ class includes a number of quasars that are variously defined as optically violently variable quasars (OVV), highly polarized quasars (HPQ), flat spectrum radio quasar (FSRQ) and core dominated quasar (CDQ). Although the names OVV, HPQ, CDQ, and FSRQ indicate different empirical definition, the common continuum emission properties of all these objects suggest that they are basically the same thing (Fugmann 1989; Impey et al. 1991; Valtaoja et al. 1992; Wills et al. 1992). In the following we will refer to all them as HPQ.

How much the distinction between BLL and HPQ is due to intrinsic properties or it is a consequence of the classification criteria remains unclear. Recent results (Padovani, Giommi & Fiore 1996; Sambruna 1997) show the X-ray spectrum of the

two classes is similar, in contrast with results found in early studies based on much less data (Worrall & Wilkes 1990; Brunner et al. 1994). A more quantitative difference is expressed by the idea that BLL and HPQ may be associated with Fanaroff & Riley radio galaxies of type I and II, respectively. Analyzing the extended radio structure of BLL, Kollgaard et al. (1992) conclude, however, that the parent population of BLL may include both FR I and II. Similar result also reported by Murphy, Browne & Perley (1993).

The main difference between HPQ and BLL remains the emission line intensities. It is important to outline here that it is common to split blazars in two groups calling BLL the one with apparently weak (small equivalent width) emission lines and HPQ the other, and then study the properties of the two classes (including emission lines). As example the 1 Jy sample of BL Lac objects was compiled requiring even that *"emission lines in the optical spectrum are weak or absent with rest frame equivalent width of the strongest line of less than 5* Å" (Stickel et al. 1991; Stickel, Fried & Kühr 1993). This implies that, although the equivalent width is a quantity depending on both lines and continuum luminosity, in the BLL class there will be, preferentially, objects with intrinsically weaker lines.

A further and not negligible complication is introduced by the emission line variability that can be very large in some cases. This makes the object classification time dependent. As an example BL Lacertae, the prototype of the BLL class, and PKS 0521-365 have (at present) lines with e.w. > 5Å (Vermeulen et al. 1995; Ulrich 1981; Scarpa, Falomo, & Pian 1995). Both these sources, early classified as BL Lacs, at present do not match the classical BL Lac definition and should be re-classified as HPQ. Similarly, HPQ can sometime appear line-less (Miller, French, & Hawley 1978; Wills et al. 1983).

The main aim of this paper is to investigate the optical spectral properties (continuum and line) of HPQ to be compared with those of BLL and LPQ. To this aim we secured optical spectrophotometric observations of several HPQ and BLL. This data set extends the sample (mainly BLL) analyzed in Falomo, Scarpa & Bersanelli (1994; in the following FSB94).

2. Observations and data analysis

Spectrophotometric optical observations of 49 blazars were obtained at the European Southern Observatory (ESO), La Silla, Chile, in July 1994 and February 1995, using the 1.5m spectrographic telescope equipped with a Boller & Chivens spectrograph. We used as a detector a CCD (Ford aerospace chip with 15μm–pixel) which covers the range 3800–9000 Å at a resolution of 3.8 Å/pixels. Standard data reduction procedures were adopted to obtain 1-dimensional wavelength calibrated extracted spectra. Spectra were calibrated in absolute flux units using several observations of spectrophotometric standard stars (Stone 1977) obtained on the same night. Fluxes have been corrected for Galactic extinction according to the interstellar extinction law of Cardelli, Clayton & Mathis (1990). The value of A_V for each objects was derived assuming R=3.09 $\pm$ 0.06 (Rieke & Lebofsky 1985), and a gas to dust ratio of $N_H/E(B-V) = 5.2 \times 10^{21}$ (Shull & Van Steenberg 1985). The Hydrogen column density was determined either interpolating the grid of the Bell Lab Survey (Stark et al. 1992) or, when available, using the accurate narrow beam ($21'$) measurement of N_H in the direction of several AGN from Elvis et al. (1989).

Table 1. Journal of observations

object [a]	date dd-mm-yy	exp sec.	m_V^b	α
0208 − 513∗	03/07/94	1200	...	-1.26 ± 0.06
	04/07/94	2400	14.4	-1.18 ± 0.04
0403 − 133∗	04/02/95	2400	17.0	-0.40 ± 0.30
0420 − 015∗	04/02/95	2400	16.8	-1.70 ± 0.30
0521 − 365	06/02/95	2400	15.4	-1.34 ± 0.20
0537 − 441	03/02/95	1800	15.3	-1.29 ± 0.04
	05/02/95	2400	15.1	-1.27 ± 0.05
	07/02/95	1800	14.7	-1.09 ± 0.04
0548 − 323	07/02/95	2400	16.3	-0.05 ± 0.20
0735 + 178	06/02/95	2400	15.7	-1.51 ± 0.08
0736 + 017	03/02/95	2364	16.1	-0.89 ± 0.15
0743 − 006∗	07/02/95	3000	17.1	-0.29 ± 0.10
0754 + 101	04/02/95	2400	15.4	-1.04 ± 0.05
0808 + 019	03/02/95	2400	18.0	-1.30 ± 0.06
0818 − 128	05/02/95	2400	16.8	-1.10 ± 0.08
0823 + 033	05/02/95	3000	17.0	-1.80 ± 0.15
0823 − 223	05/02/95	2400	15.9	-0.89 ± 0.04
0829 + 046	06/02/95	2400	15.0	-0.80 ± 0.04
0906 + 016	07/02/95	3000	17.6	-0.30 ± 0.40
1020 − 104	06/02/95	2400	17.0	-0.79 ± 0.10
1034 − 293∗	04/02/95	2400	19.1	-1.70 ± 0.15
	07/02/95	2400	18.9	-1.65 ± 0.20
1055 + 018	03/02/95	2400	17.5	-1.37 ± 0.08
1144 − 379	05/02/95	1800	17.6	-1.43 ± 0.10
1244 − 255	01/07/94	2400	19.2	-0.70 ± 0.30
1253 − 055∗	06/02/95	2400	15.9	-1.54 ± 0.06
	02/07/94	1800	14.8	-1.45 ± 0.08
1335 − 127∗	06/02/95	2400	16.3	-1.54 ± 0.10
	01/07/94	1800	...	-1.60 ± 0.30
1424 + 240∗	03/07/94	2400	15.1	-1.00 ± 0.25
1424 − 419∗	01/07/94	1800	16.7	-1.92 ± 0.12
1502 + 107∗	01/07/94	3600	18.6	-1.00 ± 0.40
1504 − 167∗	01/07/94	3600	19.8	-0.98 ± 0.50
1514 − 242	03/07/94	1800	16.0	-0.83 ± 0.30
1519 − 273	01/07/94	2486	18.0	-1.36 ± 0.20
1522 + 155∗	04/07/94	1800	19.0	-0.05 ± 0.50
1532 + 017∗	04/07/94	1800	19.0	-0.68 ± 0.45
1546 + 028∗	03/07/94	2400	16.9	-1.50 ± 0.40
1548 + 056∗	03/07/94	3600	18.6	-0.98 ± 0.40
1553 + 113	04/07/94	2400	14.1	-0.96 ± 0.15
1656 + 053∗	01/07/94	2400	16.8	-0.55 ± 0.17
1722 + 119	03/07/94	1800	14.7	-0.87 ± 0.06
1749 + 096	03/07/94	2400	17.0	-1.67 ± 0.20
1921 − 293∗	01/07/94	2400	16.0	-1.32 ± 0.12
1936 − 155∗	04/07/94	3600	19.5	-0.56 ± 0.36
1954 − 389∗	01/07/94	2400	16.9	-1.33 ± 0.12
1958 − 179∗	01/07/94	3600	19.1	-1.11 ± 0.60
2005 − 489	01/07/94	1200	13.0	-0.50 ± 0.05
2155 − 304	01/07/94	1800	12.7	-0.59 ± 0.05
2208 − 137	01/07/94	2400	17.0	-0.45 ± 0.30
2223 − 052	03/07/94	2400	17.9	-1.26 ± 0.15
2225 − 056∗	03/07/94	2700	19.0	-1.05 ± 0.30
2240 − 260	01/07/94	2400	17.7	-1.45 ± 0.12
2243 − 124∗	03/07/94	2399	17.0	-0.90 ± 0.40
2355 − 535∗	01/07/94	2400	18.4	-1.00 ± 0.45
	04/07/94	3600	18.7	-0.56 ± 0.34

[a] An asterisk indicate "new" sources.
[b] Visual magnitudes not corrected for extinction.

The journal of observations is reported in Table 1. Columns give for each source the name, the date of observation, and the exposure time in seconds. Column 4 gives the V magnitude, obtained integrating the spectra over the filter pass band. These values are not corrected for interstellar extinction. Finally, in the last column we report the optical spectral index, derived in three different ways (according with notes on table 2): fitting the

Table 2. The sample

object [a]	other name	z	A_V	Class.	$P_{max} \pm \sigma$	Ref.	$\alpha \pm \sigma$	α_{RX}	Ref.	notes[b]
0048 − 097	PKS	···	0.21	r	27.1 ± 5	14	−0.92 ± 0.27	−0.93	7	
0109 + 225	S2	···	0.27	r	17.3 ± 1.4	14	−1.02 ± 0.29	−0.86	7	
0118 − 273	PKS	0.557	0.09	r	18.7 ± 1.0	14	−1.19 ± 0.16	−0.88	7	
0138 − 097	OC-065	0.501	0.17	r	27.3 ± 1.6	14	−1.02 ± 0.09	···		
0208 − 513∗	PKS	1.003	···	r	11.5 ± 0.4	3	−1.23 ± 0.10	···		
0215 + 015	OD +026	1.72	0.21	r	11.2 ± 0.3	15	−0.72 ± 0.10	−0.93	7	c
0301 − 243	OE-202	···	0.11	r	10.6 ± 0.2	3	−1.10 ± 0.15	···		
0323 + 022	H,1H,1ES	0.147	0.50	x	3.5 ± 0.9	14	−0.25 ± 0.05	−0.54	7	g
0338 − 214	OE-263.9	···	0.16	r	15.6 ± 2.9	14	−1.35 ± 0.11	−0.92	7	
0403 − 133∗	PKS	0.571	0.21	h	4.0 ± 1.0	6	−0.4 ± 0.3	−0.94	7	f
0414 + 009	1H, 87GB	0.287	0.51	x	5.1 ± 1.4	14	−0.37 ± 0.18	−0.54	7	g
0420 − 015∗	PKS	0.915	0.56	h	20.2 ± 1.0	4	−1.7 ± 0.3	−0.91	7	
0422 + 005	PKS	···	0.42	r	23.3 ± 1.1	14	−1.37 ± 0.13	−0.87	7	
0521 − 365	ESO-362	0.055	0.21	h	6.0 ± 1.5	12	−1.24 ± 0.22	−0.80	7	g
0537 − 441	PKS	0.894	0.20	r	18.7 ± 0.5	3	−1.24 ± 0.17	−0.91	22	
0548 − 323	4U,H,1H,ES	0.069	0.14	x	1.4 ± 0.8	15	−0.42 ± 0.34	−0.56	7	g
0735 + 178	PKS	> 0.424	0.28	r	31.9 ± 1.2	16	−1.31 ± 0.13	−0.89	7	
0736 + 017	PKS	0.191	0.72	h	6.8 ± 0.8	16	−0.85 ± 0.15	−0.89	7	f
0743 − 006∗		0.994	0.30	h	1.1 ± 0.4	3	−0.29 ± 0.08	···		
0754 + 101	MRC,OI+094.4	···	0.16	r	19.0 ± 0.6	16	−1.11 ± 0.07	−0.85	7	
0808 + 019	HB89,OJ+014	···	0.25	r	14.0 ± 2.0	11	−0.81 ± 0.35	−0.81	7	
0818 − 128	OJ-131	···	0.45	r	24.7 ± 1.7	2	−0.96 ± 0.17	−0.91	7	
0823 + 033	OJ+038,PKSB	0.506	0.22	r	23.0 ± 5.7	9	−1.46 ± 0.34	−0.87	22	
0823 − 223	PKS	> 0.910	0.62	r	8.5 ± 0.4	1	−0.93 ± 0.07	···		
0829 + 046	OJ+049	0.18	0.18	r	12.0 ± 3.0	12	−0.87 ± 0.31	−0.85	7	g
0836 + 182	HB89, 87GB	···	0.19	r	15.5 ± 1.5	17	−1.58 ± 0.22	···		
0851 + 203	OJ 287	0.306	0.18	r	37.2 ± 0.4	16	−1.37 ± 0.22	−0.81	7	
0906 + 016	PKS,4C,DA263	1.018	0.22	h	7.3 ± 0.7	5	−0.3 ± 0.40	−0.90	7	c
1020 − 104	OL-13, PKS	0.197	0.30	h	···		−0.36 ± 0.26	···		f
1034 − 293∗	PKS	0.312	0.28	h	13.8 ± 1.2	1	−1.67 ± 0.20	−0.92	7	
1055 + 018	DA293,PKS,4C	0.888	0.23	h	5.0 ± 0.5	1	−1.38 ± 0.05	···		
1057 + 101	MRC, HB89	1.317	0.15	h	10 ± 2	12	−0.58 ± 0.05	···		
1101 − 232	2A,3A,4U,1H	0.186	0.34	x	7.4 ± 1.5	18	−0.48 ± 0.18	−0.52	22	g
1144 − 379	MRC. PKS	1.048	0.52	r	8.5 ± 1.7	20	−1.15 ± 0.18	−0.86	23	
1244 − 255	HB89, PKS	0.663	0.42	h	11.2 ± 2.7	9	−0.95 ± 0.24	···		
1253 − 055∗	3C 279	0.536	0.13	r	43.3 ± 0.7	14	−1.50 ± 0.08	−0.92	7	
1309 − 217	HB89, MC1	1.498	0.49	r	···	3	−1.20 ± 0.12	···		
1335 − 127∗		0.541	0.24	h	···		−1.54 ± 0.10	···		
1400 + 162	VRO 16.14.01	0.245	0.10	r	14.0 ± 2.8	18	−1.38 ± 0.05	−0.81	7	
1402 + 044	1E, MS	···	0.13	x	9.5 ± 0.5	4	−1.06 ± 0.23	−0.65	7	
1407 + 022	OQ+012, PKS	···	0.16	r	···		−1.18 ± 0.12	···		
1424 + 240∗	PG	···	0.16	r	5.1 ± 0.6	2	−1.00 ± 0.25	−0.79	7	
1424 − 419∗	PKS	1.522	···	h	6.6 ± 0.3	3	−1.92 ± 0.12	···		
1502 + 107∗	PKS	1.833	0.13	h	19.8 ± 1.8	1	−1.0 ± 0.40	···		
1504 − 167∗	PKS	0.876	0.47	h	5.3 ± 0.7	3	−0.98 ± 0.50	−0.95	10	
1514 − 242	AP Lib	0.049	0.52	r	6.9 ± 1.3	14	−1.07 ± 0.17	−0.90	7	g
1519 − 273	PKS	> 0.2	0.55	r	11.4 ± 0.6	3	−1.36 ± 0.20	−0.87	23	
1522 + 155∗		0.628	0.16	h	12.5 ± 1.2	6	−0.05 ± 0.50	−0.91	7	
1532 + 017∗		1.420	0.29	h	5.0 ± 1.2	9	−0.68 ± 0.45	···		
1538 + 149	4C 14.60, PKS	0.605	0.19	r	29.6 ± 0.7	15	−1.70 ± 0.13	−0.91	7	
1546 + 028∗	PKS	0.412	0.40	h	4.1 ± 0.6	6	−1.5 ± 0.4	···		f
1548 + 056∗	PKS	1.422	0.26	r	4.7 ± 0.1	3	−0.98 ± 0.40	···		
1553 + 113	PG	···	0.21	x	···		−0.90 ± 0.08	−0.64	22	
1656 + 053∗	PKS	0.879	0.36	h	3.3 ± 0.6	1	−0.55 ± 0.17	···		
1722 + 119	H, 4U, 87GB	···	0.51	x	15.5 ± 0.4	4	−1.03 ± 0.14	−0.57	22	
1749 + 096	OT+081	0.322	0.57	h	31.3 ± 0.6	8	−1.27 ± 0.33	−0.87	7	g
1921 − 293∗		0.352	0.48	h	···		−1.32 ± 0.12	−0.94	7	
1936 − 155∗		1.657	0.56	h	12.2 ± 3.4	3	−0.56 ± 0.36	···		
1954 − 389∗	PKS	0.626	0.39	h	10.9 ± 0.3	3	−1.33 ± 0.12	···		
1958 − 179∗	PKS	0.65	0.46	h	25.3 ± 1.1	1	−1.11 ± 0.61	···		
2005 − 489	PKS, 1ES	0.071	0.33	x	2 ± 0.2	17	−0.79 ± 0.17	−0.59	22	
2012 − 017	PKSB, PKS	···	0.52	r	···		−1.63 ± 0.12	···		
2155 − 304	PKS,1H,2A,3A	0.116	0.11	x	10.3 ± 0.3	14	−0.61 ± 0.08	−0.57	7	
2201 + 044		0.028	0.29	r	···	15	−1.29 ± 0.6	−0.80	21	g
2208 − 137	PKS	0.392	0.20	h	8.7 ± 0.4	6	−0.45 ± 0.30	···		f
2223 − 052	3C 446	1.404	0.33	h	13.6 ± 0.4	14	−1.39 ± 0.22	−0.84	10	
2225 − 056∗	PHL 5200	1.981	0.30	h	4.1 ± 0.8	13	−1.05 ± 0.3	···		a
2230 + 115	PKS	1.037	0.36	h	10.9 ± 0.3	6	−0.29 ± 0.43	−0.90	10	
2240 − 260	OY-268, PKS	0.774	0.09	r	15.1 ± 0.5	3	−1.54 ± 0.12	−0.93	23	
2243 − 124∗	PKS	0.630	0.31	h	5.0 ± 0.3	1	−0.9 ± 0.4	···		f
2254 + 074	OY+091, MG	0.190	0.32	r	20.4 ± 0.5	15	−1.25 ± 0.29	−0.87	7	g
2355 − 535∗	PKS	1.006	···	h	3.7 ± 0.6	3	−0.70 ± 0.34	···		
2356 − 309	U, 4U	0.165	0.08	x	···		−1.85 ± 0.07	···		g

[a] An asterisk indicate the "new" sources not presented in Falomo Scarpa Bersanelli 1994.

[b] Notes are as follow: **a** indicates the source is a broad absorption line quasar, **c** indicates the spectrum is "complex" and only marginally compatible with a power law model, **f** indicates the presence of relevant FeII emission lines and Balmer continuum, and **g** indicates the host galaxy stellar emission was detected.

Table 2. (continued) References

1	Wills et al. 1992
2	Ballard et al. 1990
3	Impey & Tapia 1990
4	Jannuzi & Smith 1994
5	Moore & Stockman 1984
6	Moore & Stockman 1981
7	Ledden & O'Deel 1985
8	Brindel et al. 1986
9	Impey & Tapia 1988
10	Padovani 1992
11	Kinman 1976
12	Angel & Stockman 1980
13	Stockman & Angel 1978
14	Mead et al. 1990
15	Brindle et al. 1991
16	Smith et al. 1987
17	Wills et al. 1980
18	Zekl et al. 1981
19	Fugmann & Meisenheimer 1988
20	Kühr & Schmidt 1990
21	Ghisellini et al. 1986
22	Giommi Ansari & Micol 1995
23	Sambruna 1995

spectrum with a simple power law model; fitting a two components model: power law plus the emission from a typic elliptical galaxy (Yee & Oke 1978) if it is relevant; fitting with a power law only the region redward of H_β , when the presence of FeII emission lines has been detected.

Data in table 1 have been joined with data reported by FSB94, obtaining a sample of 73 blazars, which have been selected from the lists of Angel & Stockman (1980), Moore & Stockman (1981), Wills et al. (1992), and Veron-Cetty & Veron (1993). The only criteria for selecting objects being observability from La Silla and detectability at the 1.5m telescope. This constrain correspond roughly to a cutoff at $m_V \sim 20$ and $\delta < +25$. The entire sample includes 30 HPQ and 43 BLL. Despite previous classifications, in the following analysis we reclassified all sources defining as BLL the objects for which the emission lines rest frame e.w. was, at the moment of observation, smaller than 5 Å. This operational definition introduced by Moore & Stockman (1981) is not free from criticism, but has been largely applied in the past to define samples of BLL successively used to determinate their line intensity. Our and previous classification agree in all cases with that reported in the source lists but for 3c 279, which shows in our spectra very weak lines, and PKS 0521-365 that show strong lines. This criterium of classification (e.w.$<$ 5 Å) is adopted here in order to address the bias introduced when studying line intensities.

Considering that BLL are classically divided in two different groups based on their selection criteria, the 43 BLL in our sample include 10 X-ray selected (XBL) and 33 radio selected (RBL) objects. Classification of RBL and XBL is mainly based on literature search and it is well consistent, for the objects with measured x-ray fluxes, with the classical $\alpha_{rx} = -0.75$ separation criteria (Ledden & O'Dell 1985; Padovani & Giommi 1995) as is also clearly visible in Fig. 3.

These two subclasses differ in a systematic way, RBL having a flatter energy distribution at all frequencies (Ghisellini et al. 1986; Giommi, Ansari & Micol 1995). It is worth to note that recently RBL and XBL has been called respectively Low energy cut off (LBL) and High energy cut off (HBL) to give a more direct indication of the different broad–band flux energy distribution observed in these two classes (see Giommi, Ansari & Micol 1995). These different names refer substantially to the same objects.

The whole sample is summarized in Table 2. Columns give: 1) the coordinate name; 2) other names or catalogue; 3) redshift; 4) the adopted interstellar extinction (A_V) in magnitudes; 5) the classification: x for XBL, r for RBL and h for HPQ; 6) maximum observed optical polarization (from the literature). This data are quite heterogeneous and for several sources only one measurement is available; 7) reference for polarization; 8) the optical spectral index of the non thermal component; 9) the radio to X-ray spectral index; 10) reference for column 9.

3. Results

3.1. The optical spectra

We present in Fig. 1 a representative optical spectrum of each source not previously reported by FSB94. As a whole, selected sources show preferentially a non thermal continuum, with several cases of featureless spectrum.

The optical flux distribution of the BLL subsample (43 objects) is remarkably smooth and well described by a power law model. Most of the objects show a true featureless continuum (indeed for 15 sources the redshift is unknown), while others exhibit, superimposed on a featureless continua, the signature of thermal emission from the host galaxy. In all cases where the host emission was detected (10 BLL and 1 HPQ), a good description of the spectrum is achieved by decomposing the spectrum into a non-thermal power law continua plus the emission of an elliptical galaxy (see FSB94).

On the other hand, in the HPQ subsample (30 sources) most of the spectra show strong permitted and forbidden emission lines, as normally observed in LPQ but, at variance from LPQ, in 23 of 30 cases the continuum is compatible with a simple power-law model. This confirms the preliminary results of Rieke, Lebofsky & Kinman (1979) and Moore & Stockman (1984), which found the HPQ continua is more smooth than that of LPQ.

Of the remaining sources, in six cases (0403-133, 0736+017, 1020-104, 1546+02, 2208-137, 2243-124) we clearly detect the presence of FeII emission lines and/or the Balmer continuum emission. As shown by photoionization models, in these cases blueward of H_β the spectrum may be described by two components: a power law nonthermal continuum, and the emission from blended Fe II lines plus the Balmer continuum (e.g. Wills 1986). We therefore fitted a power law model only to the redder region of the spectrum, which is not affected by these additional emissions. The spectral index derived for these six sources is not different from the values found for the other HPQ (see in Table 2).

In two objects (0906+016 and 2230+115) the spectrum is rather complex and significant departures from a power law are

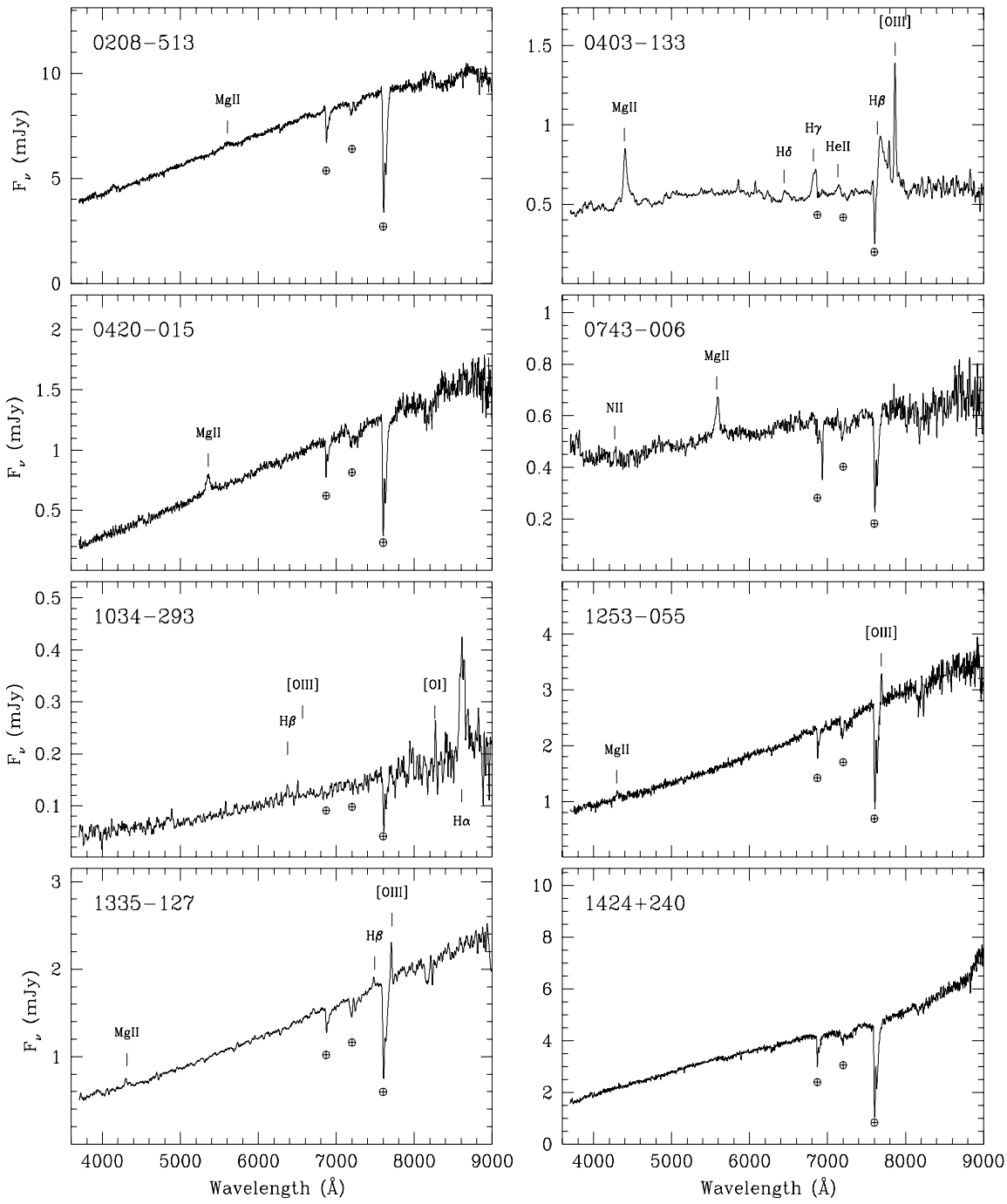

Fig. 1. The optical spectrum of program objects not previously reported in FSB94. Spectra are represented in the λ, F_λ plane. In this plot the flux was not corrected for interstellar extinction. Atmospheric absorption bands ($\oplus$) and main features are marked.

found. As a consequence, the reported spectral index must be considered with caution.

3.2. The distribution of the optical spectral indices

The average optical spectral index for the whole sample of blazars is $\alpha_O = -1.00 \pm 0.09$. The distribution of α_O for the BLL and HPQ subsamples, reported in Fig. 2, are rather similar and indeed the two groups have the same mean value of $< \alpha_{HPQ} >= -1.01 \pm 0.17$ and $< \alpha_{BLL} >= -0.99 \pm 0.11$ (quoted errors are the 95% confidence interval). This data give a statistically significant confirmation of the fact that blazars have in general steeper optical spectral energy distribution than LPQ, which have a median index of $\alpha_O \sim -0.5$ (Moore & Stockman 1984) or even flatter (Francis 1996), confirming also

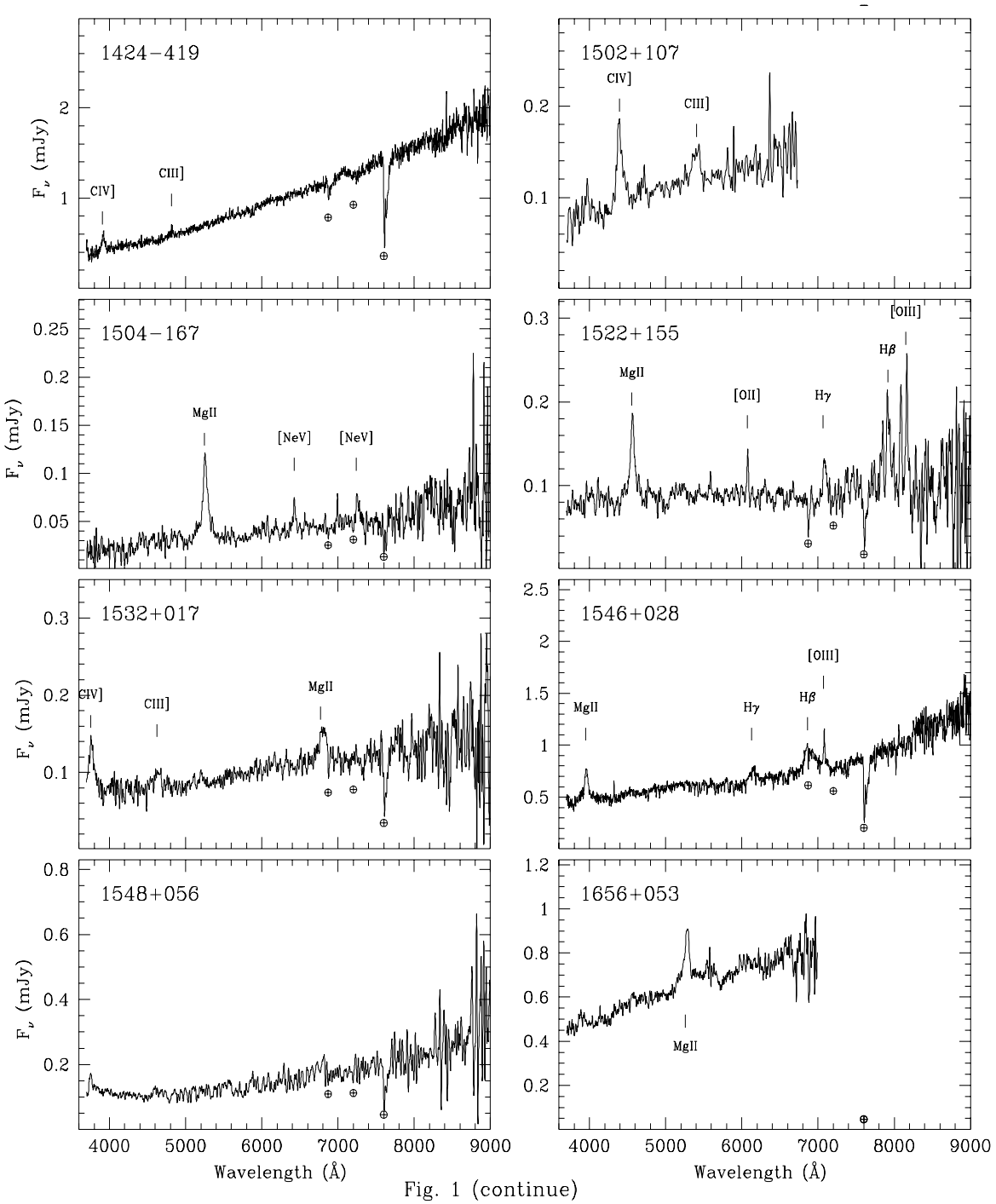

Fig. 1. (continued)

the suggested connection between high polarization and steep optical continua (Oke, Neugebauer & Becklin 1969).

It is interesting to compare the shape of the spectral index distributions for HPQ and BLL subsamples. The BLL distribution is characterized by the presence of a secondary peak around $\alpha = -0.4$ (see Fig. 2). This is clearly due to the presence of the X-ray selected sources that cluster toward flatter spectral indices. In fact, as previously found by a number of authors (c.f. Ghisellini et al. 1986; FSB94), RBL and XBL have different spectral index distributions over various frequencies. Our average for the two subsamples being respectively $< \alpha_{RBL} >= -1.23 \pm 0.08$ and $< \alpha_{XBL} >= -0.49 \pm 0.20$ (errors are 95% confidence level). To this regard we note, however, that since different techniques may tend to pick out more extreme XBL and RBL, there could be a smoother continuity between the two subclasses as suggested by other investigations (Nass et al. 1996).

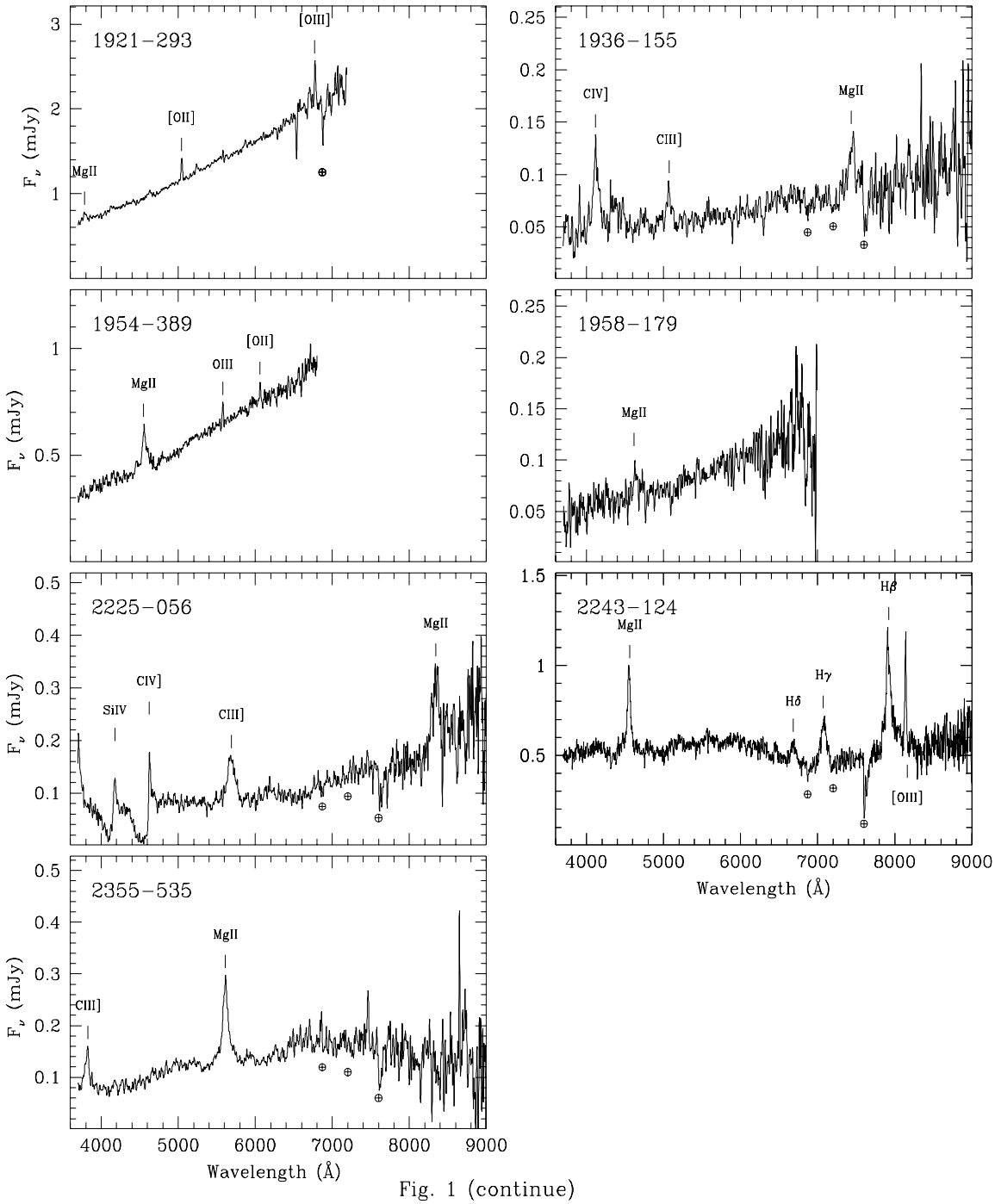

Fig. 1 (continue)

Fig. 1. (continued)

The distribution for HPQ is less peaked and may also suggest a secondary maximum at flatter indices. Because of the small number of objects considered we can not exclude that it may be a statistical fluctuation. Anyway it is worth to investigate if it could reflect the existence of two different populations of HPQ, similarly to RBL and XBL.

To clarify this point, we plot the objects in the $\alpha_o - \alpha_{RX}$ plane (see Fig 3). In this representation (Ledden & O'Dell 1985) RBL and XBL tend to occupy well distinct regions and one could expect HPQ do the same. We found, however, that all HPQ clustered in the same region together with RBL. The clear separation of all HPQ from XBL suggests that, with respect to the overall energy distribution, only one type of HPQ exists.

On the other hand the cumulative distributions of α_o for RBL and HPQ appear to be different at 99.9% confidence level based on a KS–test (see Fig. 4). It remains therefore unclear why a number of HPQ exhibit flat optical spectral index.

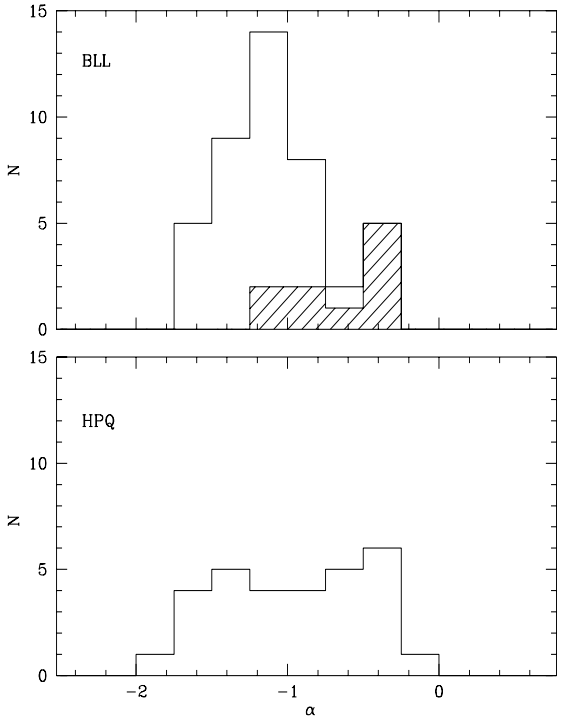

Fig. 2. Distribution of optical spectral indices. Upper panel reports the distribution for BLL. The radio selected (33 objects) and the X-ray selected objects (10 objects; *shaded area*) are shown separately. Lower panel reports the HPQ (30 objects).

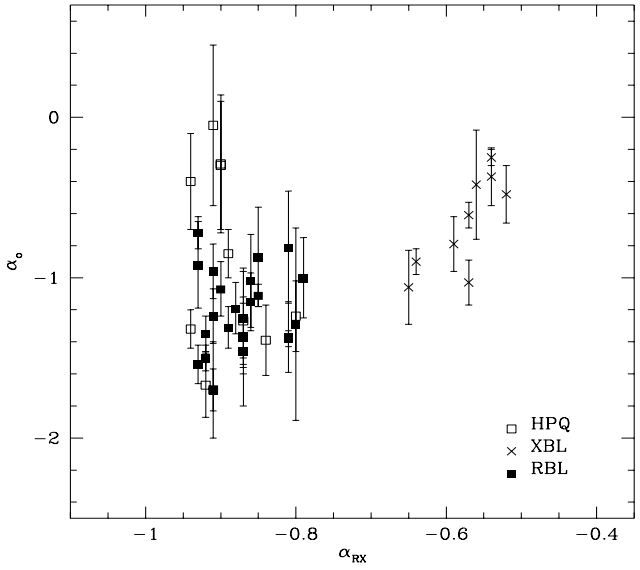

Fig. 3. The optical spectral index is plotted versus radio-to-x-ray spectral index, computed for most objects from 5 GHz and 1 KeV. Highly polarized quasars and RBL clustered together while XBL are clearly separated. The absence of HPQ in the region filled by XBL indicate that there are not HPQ with XBL like energy distribution.

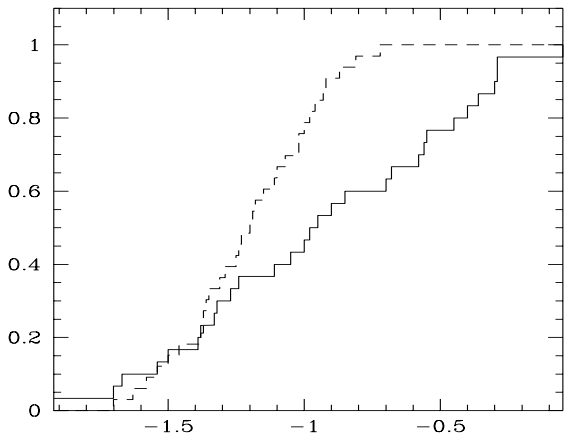

Fig. 4. Cumulative distribution for the optical spectral index of HPQ (solid line) and RBL (dashed line). The two distributions differ at the 95% significance level.

3.3. Optical spectral indices versus redshift

For 58 objects out of 73 observed we know the redshift either from absorptions in the host galaxy or from detection of emission lines. The sources span a relatively large interval in redshift: $0.028 < z < 1.98$. This enable us to investigate if a variation of α_o is induced by different redshift since we are observing different regions of the rest frame emission.

We did not found any evident correlation between redshift and α_O (see Fig. 5) both for HPQ and BLL. Also objects without redshift do not show any preferential value of α_O . The absence of correlation indicates that the same spectral index apply at different wavelength. This finding is consistent with the results reported for a sample of BLL by Pian et al. 1994, who found that a single power low describes the whole near-IR–optical–UV spectra or, in other words, that significant curvature of the spectrum induced by synchrotron losses may occur at lower or higher frequencies.

3.4. Spectral index versus polarization

The high optical polarization is one of the characteristic properties of the blazars class. To investigate how the polarization level is related with other optical properties, we gathered from the literature for each source optical polarization data. Data were found for 90% of the objects in Table 2. Since for many objects just one measurement was found we chose to use the maximum observed polarization (P_{max}). Using the average polarization does not significantly change the discussion below.

The cumulative distributions of P_{max} for BLL and HPQ indicates that the latter are on average less polarized (Fig. 6). Indeed, in most cases the maximum observed value for HPQ being under 15%. We note, however, that this difference could be due to the fact that BL Lac objects have been more largely monitored for polarization than HPQ, therefore it is more likely that they have been observed in a larger polarization state.

When P_{max} is plotted versus the optical spectral index, HPQ and BLL show rather similar behavior (see Fig. 7a). The level of polarization tends to be correlated with the spectral index,

Table 3. Emission lines properties.

object	Line Identification	e.w. (Å)	Flux[a] $10^{-16} ergs^{-1} cm^2$	e.w. rest frame (Å)	Luminosity[b] 10^{40} erg s^{-1}
0208 − 51	Mg II 2798	5 ± 5	180 ± 160	2.5 ± 2.5	1.75 ± 1.6 × 10^4
0403 − 13	Mg II 2798	54 ± 12	410 ± 86	34 ± 7	1.22 ± .26 × 10^4
	[OII] 3727-29	3.6 ± 1.1	18 ± 5.5	2.3 ± 0.7	4.98 ± 1.5 × 10^2
	[NIII] 3869	2.6 ± 1	12 ± 5	1.65 ± 0.6	3.30 ± 1.4 × 10^2
	Hδ	8 ± 2	31 ± 7	5.1 ± 1.3	8.42 ± 1.9 × 10^2
	Hγ	18.6 ± 3	66 ± 9	11.8 ± 1.9	1.77 ± .24 × 10^3
	HeII 4541	5 ± 2	17 ± 7	3.2 ± 1.3	4.53 ± 1.9 × 10^2
	Hβ	61 ± 6	177 ± 17	38.8 ± 3.8	4.64 ± .45 × 10^3
	[OIII] 4959	6 ± 0	22 ± 0	3.8 ± 1.3	5.7 ± 2 × 10^2
	[OIII] 5007	42 ± 5	121 ± 10	26.7 ± 3.2	3.15 ± .26 × 10^3
0420 − 01	MgII 2798	19.3 ± 3.7	129 ± 23	10.1 ± 1.9	1.68 ± .30 × 10^4
0521 − 36	[OII] 3726	5.6 ± 0.5	140 ± 9	5.3 ± 0.5	2.56 ± .16 × 10^1
	[OIII] 4363+Hγ	2.5 ± 0.5	90 ± 15	2.4 ± 0.5	1.57 ± .26 × 10^1
	Hβ	1.72 ± 0	52 ± 0	1.6 ± 0.6	8.79 ± 3 × 10^0
	[OIII] 5007	5.0 ± 0	144 ± 0	4.74 ± 0.10	2.42 ± 1 × 10^1
	[OI] 6300	2.0 ± 0.16	61 ± 5	1.90 ± 0.15	9.77 ± 0.8 × 10^0
	Hα Broad+Narrow	27.6 ± 1	646 ± 2	26.2 ± 0.95	1.03 ± 0.03 × 10^2
	[NII] 6583	0.89 ± 0.2	33 ± 5	0.84 ± 0.19	5.24 ± 0.8 × 10^0
	[SII] 6716-32	1.17 ± 0	61 ± 0	∼ 1.1	∼ 9.64
0537 − 44	MgII 2798	2.2 ± 0.7	59 ± 19	1.16 ± 0.37	5.18 ± 1.7 × 10^3
0736 + 01	Hδ	6 ± 2	8 ± 3	5.0 ± 1.7	2.65 ± 1.0 × 10^1
	Hγ	11.6 ± 0.7	148 ± 7	9.7 ± 0.6	4.70 ± .22 × 10^2
	Hβ	27 ± 3	333 ± 25	22.8 ± 2.5	9.91 ± .74 × 10^2
	[OIII] 5007	4.2 ± 0.5	51 ± 5	3.5 ± 0.4	1.50 ± .15 × 10^2
	Hα	138 ± 7	1410 ± 44	116 ± 6	3.59 ± .11 × 10^3
0743 − 00	NII 2141	3.7 ± 1	30 ± 8	1.9 ± 0.5	4.16 ± 1.1 × 10^3
	MgII 2798	19 ± 5	115 ± 24	9.5 ± 2.5	1.43 ± .30 × 10^4
0906 + 01	CIII] 1909	23 ± 5	133 ± 26	11.4 ± 2.5	1.83 ± .36 × 10^4
	MgII 2798	47 ± 12	148 ± 36	23 ± 6	1.79 ± .44 × 10^4
1020 − 10	[NeV] 3426	4.4 ± 2.4	37 ± 19	3.7 ± 2.0	1.09 ± .56 × 10^2
	[NeIII] 3869	3.6 ± 1.2	23 ± 7	3.0 ± 1.0	6.44 ± 2.0 × 10^1
	Hγ Broad+Narrow	41 ± 5	204 ± 20	34.2 ± 4.2	5.46 ± .54 × 10^2
	Hβ Broad	136 ± 10	562 ± 20	114 ± 8	1.45 ± .052 × 10^3
	Hβ Narrow	2.9 ± 1	22 ± 5	2.4 ± 0.8	5.68 ± 1.3 × 10^1
	[OIII] 4959	13 ± 2	80 ± 4	10.9 ± 1.7	2.05 ± .10 × 10^2
	[OIII] 5007	44 ± 2	240 ± 5	36.8 ± 1.7	6.15 ± .12 × 10^2
	Hα Narrow	1.25 ± 0.25	20 ± 3	1.04 ± 0.21	4.74 ± .71 × 10^1
	Hα Broad	705 ± 40	2480 ± 55	589 ± 33	5.88 ± .13 × 10^3
1034 − 29	Hβ	8.3 ± 1.6	7.4 ± 1.2	6.3 ± 1.2	5.14 ± .83 × 10^1
	[OIII] 4959	5.4 ± 1.5	4.7 ± 1.1	4.1 ± 1.1	3.25 ± .76 × 10^1
	[OIII] 5007	13.4 ± 1.7	11.6 ± 1.2	10.2 ± 1.3	8.00 ± .83 × 10^1
	[OI]+[SIII] 6300	5.4 ± 2	5 ± 2.5	4.1 ± 1.5	3.23 ± 1.6 × 10^1
	Hα	84 ± 20	108 ± 17	64 ± 15	6.89 ± 1.1 × 10^2
1055 + 01	MgII 2798	12 ± 3	44 ± 9	6.4 ± 1.6	3.89 ± .79 × 10^3
1057 + 10	CIII] 1909	14 ± 2.3	63 ± 10	6.0 ± 1.0	4.89 ± .82 × 10^4
	MgII 2798	23 ± 5	62 ± 10	9.9 ± 2.2	1.42 ± .22 × 10^4
1144 − 37	MgII 2798	5.9 ± 1.7	18 ± 5	2.9 ± 0.8	3.11 ± .86 × 10^3
1244 − 25	MgII 2798	53 ± 7	240 ± 30	32 ± 4	1.31 ± .16 × 10^4
	[OII] 3727	11 ± 4	6 ± 2	6.6 ± 2.4	2.83 ± .94 × 10^2
	[NeIII] 3869	13 ± 4	6.3 ± 2	7.8 ± 2.4	2.93 ± .93 × 10^2
	Hδ Broad+Narrow	17 ± 8	1.5 ± 3	10.2 ± 4.8	6.82 ± 14 × 10^1
	Hγ Broad+Narrow	39 ± 10	16 ± 4	23.5 ± 6.0	7.11 ± 1.8 × 10^2
	Hβ Broad+Narrow	60 ± 20	23 ± 8	36 ± 12	9.71 ± 3.4 × 10^2
1253 − 05	MgII 2798	5.3 ± 2.0	90 ± 38	3.4 ± 1.3	2.1 ± 0.8 × 10^3
	[OIII] 5007	3.8 ± 0.8	50 ± 10	2.5 ± 0.5	1.07 ± .21 × 10^3
1335 − 12	MgII 2798	8 ± 2	63 ± 11	5.2 ± 1.3	1.73 ± .30 × 10^3
	Hβ	1.9 ± 0.3	14 ± 3	1.23 ± 0.19	3.30 ± .71 × 10^2
	[OIII] 5007	4.1 ± 0.5	31 ± 4	2.66 ± 0.32	7.24 ± .93 × 10^2

Table 3. (continued) Emission lines properties.

object	Line Identification	e.w. (Å)	Flux[a] $10^{-16} ergs^{-1}cm^2$	e.w. rest frame (Å)	Luminosity[b] 10^{40} erg s^{-1}
1424 − 41	CIV] 1550	21 ± 4	168 ± 23	8.3 ± 1.6	5.18 ± .71 × 10^4
	CIII] 1909	4.2 ± 0.6	31 ± 5	1.67 ± 0.24	9.56 ± 1.5 × 10^3
1502 + 10	CIV] 1550	91 ± 12	129 ± 12	32 ± 4	8.01 ± .75 × 10^4
	CIII] 1909	30 ± 4	36 ± 4	10.6 ± 1.4	2.15 ± .24 × 10^4
1504 − 16	MgII 2798	240 ± 77	85 ± 16	128 ± 41	9.14 ± 1.7 × 10^3
	[NeV] 3426	25 ± 8	8 ± 2	13.3 ± 4.3	7.83 ± 2.0 × 10^2
	[NeIII] 3869	17 ± 5	5 ± 1	9.1 ± 2.7	4.63 ± .92 × 10^2
1522 + 15	MgII 2798	95 ± 21	116 ± 20	58 ± 13	4.09 ± .70 × 10^3
	[OII] 3727-29	13 ± 4	10 ± 3	8.0 ± 2.5	3.33 ± 1.0 × 10^2
	Hγ	28 ± 9	14 ± 4	17.2 ± 5.5	4.56 ± 1.3 × 10^2
	Hβ	32 ± 7	15 ± 5	19.7 ± 4.3	4.80 ± 1.6 × 10^2
	[OIII] 5007	39 ± 11	17 ± 3	24 ± 7	5.41 ± .95 × 10^2
1532 + 01	CIV] 1550	87 ± 10	130 ± 30	36.0 ± 4.1	4.95 ± 1.1 × 10^4
	CIII] 1909	28 ± 15	32 ± 15	11.6 ± 6.2	1.13 ± .52 × 10^4
	MgII 2798	40 ± 10	30 ± 6	16.5 ± 4.1	9.36 ± 1.9 × 10^3
1546 + 02	MgII 2798	53 ± 13	468 ± 100	37.5 ± 9	8.55 ± 1.8 × 10^3
	Hγ	16 ± 6	82 ± 27	11.3 ± 4.3	1.20 ± .40 × 10^3
	Hβ	44 ± 8	208 ± 30	31 ± 6	2.93 ± .42 × 10^3
	[OIII] 5007	14 ± 3	63 ± 10	9.9 ± 2.1	8.76 ± 1.4 × 10^2
1656 + 05	MgII 2798	34 ± 8	242 ± 55	18.1 ± 4.3	2.35 ± .54 × 10^4
1749 + 09	Hβ	3.5 ± 1	20 ± 6	2.65 ± 0.76	1.87 ± .56 × 10^2
	[OIII] 5007	1.7 ± 0.5	10 ± 2.5	1.29 ± 0.38	9.18 ± 2.3 × 10^1
	Hα	22 ± 8	146 ± 54	16.6 ± 6.0	1.14 ± .42 × 10^3
1921 − 29	MgII 2798	7 ± 3	90 ± 25	5.2 ± 2.2	1.30 ± .36 × 10^3
	[OII] 3727+29	4.6 ± 0.5	63 ± 7	3.40 ± 0.37	7.57 ± .84 × 10^2
	[OIII] 5007	5 ± 1.5	65 ± 12	3.7 ± 1.1	6.76 ± 1.2 × 10^2
1936 − 15	CIV] 1550	152 ± 57	125 ± 28	57 ± 21	1.03 ± .23 × 10^5
	CIII] 1909	47 ± 11	28 ± 5	17.7 ± 4.1	1.95 ± .35 × 10^4
	MgII 2798	44 ± 13	20 ± 5	16.6 ± 4.9	1.12 ± .28 × 10^4
1954 − 38	MgII 2798	25 ± 5	159 ± 23	15.4 ± 3.1	7.27 ± 1.1 × 10^3
	OIII 3430	2.5 ± 0.5	16 ± 3	1.54 ± 0.31	6.60 ± 1.2 × 10^2
	[OII] 3727	2.1 ± 0.6	13 ± 4	1.29 ± 0.37	5.20 ± 1.6 × 10^2
1958 − 17	MgII 2798	21 ± 5	19 ± 4	12.7 ± 3.0	1.02 ± .21 × 10^3
2201 + 04	[OIII] 5007	2.2 ± .5	34 ± 4	2.15 ± 0.4	2.15 ± .2 × 10^3
	[OI] 6300	2.0 ± .5	35 ± 5	1.95 ± 5.0	1.9 ± .19 × 10^3
	Hα narrow	3.5 ± .5	75 ± 10	3.4 ± 0.5	4.0 ± .7 × 10^3
	[NII] 6584	3.5 ± .6	75 ± 12	3.4 ± 0.6	4.0 ± .9 × 10^3
2208 − 13	MgII 2798	63 ± 7	733 ± 7	45.3 ± 5.0	9.11 ± .09 × 10^3
	Hϵ	3.3 ± 1	16 ± 5	2.4 ± 0.7	1.81 ± .57 × 10^2
	Hδ	9.5 ± 2	43 ± 10	6.8 ± 1.4	4.84 ± 1.1 × 10^2
	Hγ	31 ± 3	131 ± 12	22.3 ± 2.2	1.46 ± .13 × 10^3
	Hβ	85 ± 5	307 ± 13	61.1 ± 3.6	3.35 ± .14 × 10^3
	[OIII] 5007	26 ± 2	89 ± 4	18.7 ± 1.4	9.65 ± .43 × 10^2
2223 − 05	CIII] 1909	25 ± 10	73 ± 28	10.4 ± 4.2	2.56 ± .98 × 10^4
	MgII 2798	39 ± 12	90 ± 25	16.2 ± 5.0	2.76 ± .77 × 10^4
2225 − 05	SiIV or OIV 1401	36 ± 9	40 ± 7	12.1 ± 3.0	3.94 ± .69 × 10^4
	band at 4100	79 ± 9	91 ± 19	26.5 ± 3.0	9.03 ± 1.9 × 10^4
	band at 4528	163 ± 7	180 ± 20	54.7 ± 2.4	1.71 ± .20 × 10^5
	CIV] 1550	33 ± 6	35 ± 4	11.1 ± 2.0	3.29 ± .38 × 10^4
	CIII] 1909	115 ± 22	91 ± 12	38.6 ± 7.4	7.92 ± 1.0 × 10^4
	MgII 2798	54 ± 15	47 ± 8	18.1 ± 5.0	3.65 ± .62 × 10^4
2230 + 11	MgII 2798	51 ± 12	220 ± 60	25.0 ± 5.9	3.22 ± .88 × 10^4
2243 − 12	Mg II 2798	37 ± 6	300 ± 33	22.7 ± 3.6	1.27 ± .14 × 10^4
	Hϵ	5.5 ± 2	19 ± 5	3.37 ± 1.2	7.10 ± 1.9 × 10^2
	Hδ	13 ± 3	41 ± 8	8.0 ± 1.8	1.50 ± .29 × 10^3
	Hγ	46 ± 6	125 ± 14	28.2 ± 3.7	4.55 ± .51 × 10^3
	Hβ	103 ± 12	254 ± 21	63 ± 7	8.91 ± .74 × 10^3
	[OIII] 5007	28 ± 4	69 ± 8	17.1 ± 2.5	2.40 ± .28 × 10^3
2355 − 53	CIII] 1909	110 ± 30	136 ± 30	55 ± 14	1.33 ± .29 × 10^4
	MgII 2798	116 ± 20	142 ± 17	58 ± 10	1.39 ± .17 × 10^4

[a] Fluxes not corrected for A_V.

[b] Luminosity corrected for A_V and computed assuming H_0=50 km/s/Mpc and q_0=0

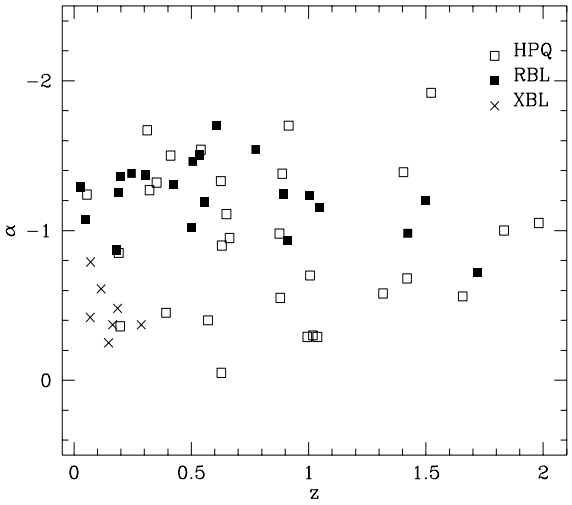

Fig. 5. The optical spectral index plotted versus distance (z). Values of α_O appear randomly distributed, without any evident correlations with z. Also the more distant sources have rather normal values of the spectral index.

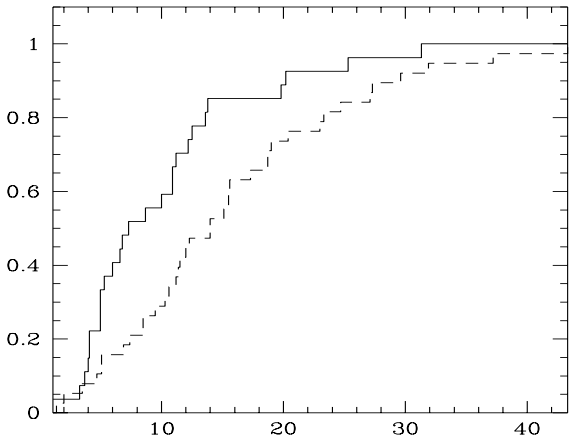

Fig. 6. Cumulative distribution for the optical polarization (maximum observed) in BL Lacs (dashed line) and in HPQ (solid line). The two distributions are different at 99% significance level.

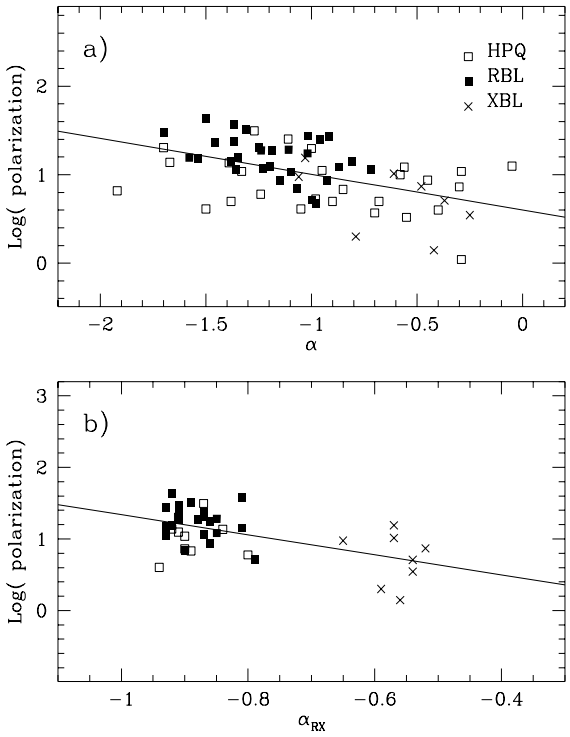

Fig. 7a and b. Upper panel reports the logarithm of maximum optical polarization versus the optical spectral index. The HPQ have a rather uniform distribution both in α_O and polarization, while the RBL show preferentially larger values of polarization compared with the XBL. A significant correlation between α_O and P_{max} is observed with the largely polarized object having the steeper continuum. Lower panel: as for upper panel but abscissa reports the radio–to–X-ray spectral index. Also in this case the two quantities appear to be correlated (see text).

with the steepest sources at highest polarization. The regression line is $Log(P_{max}) = (-0.40 \pm 0.08) \times \alpha_o + (0.6 \pm 0.10)$ with a Spearman rank correlation coefficient of -0.50. The probability of correlation is $> 99\%$, despite the relatively large spread of data around the regression line, which can be due to the well known large variability of the polarization. A similar correlation is found considering the radio–to–X-ray spectral index (α_{RX}; Fig. 7b). In this case the rank Spearman correlation coefficient is larger (-0.56) with probability $> 99\%$ for the two quantities to be correlated. In both diagrams XBL are found at the lowest levels of polarization and consequently with flatter spectral indices.

The observed $\alpha - P_{max}$ correlation does not have a simple explanation. The weak wavelength dependence of polarization (Brindle et al. 1986; Jannuzi et al. 1994) does not seem able to explain this correlation. In fact, since polarization normally increases with frequency one would expect to find larger optical polarization for objects with flatter spectral flux distributions and/or higher redshift. While no dependence on redshift is found from our data, a larger polarization is observed in the steeper sources (contrary to the expectation from the wavelength dependence of polarization). A lower overall polarization is expected in sources with conspicuous host galaxy contribution. We note, however, that the objects on the right side of Fig. 7a have not on average conspicuous host galaxies. Anyway, this effect should not influence the data in Fig. 7b.

3.5. Emission lines properties

We detected emission lines in 36 of the 73 observed sources. Data for emission lines are given in Table 3. Column report the measured lines equivalent width (e.w.; column 3), the total flux (column 4), the rest frame equivalent width (column 5) and the line luminosity (column 6). When more than 1 spectrum was available the average value is reported. The quoted errors are calculated as the difference between the line strength measured with respect to two different continuum levels, placed 1σ above and below the best estimated continuum. When several measurements of the same line were available, the weighted av-

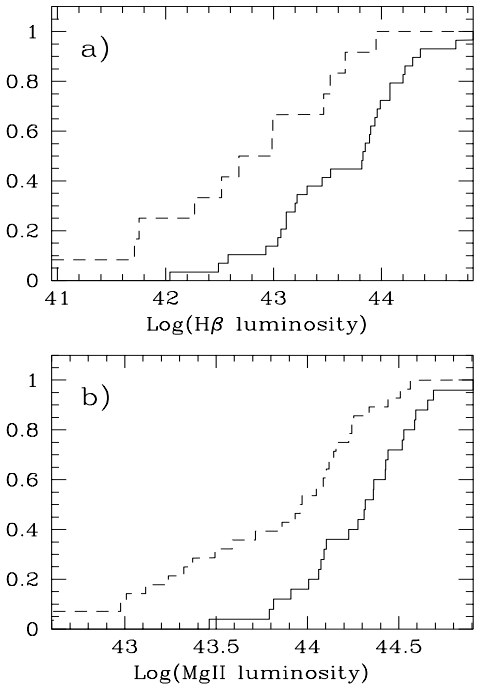

Fig. 8a and b. Comparison of emission line luminosities for blazars (dashed line) and low polarization quasars (solid line) by Yee 1980. Upper panel reports the comparison for H_β , and the lower panel for the MgII (2798). In both cases low polarization quasars show, on average, significantly stronger lines.

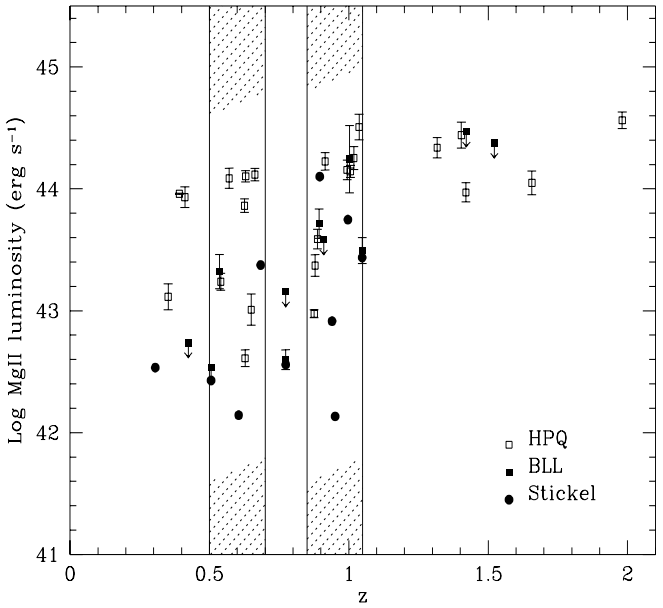

Fig. 9. The MgII 2798 Å luminosity versus redshift. Some correlation between luminosity and z induced by selection effects is present. The four vertical lines select two regions including objects at approximately the same distance (see text). Within these regions the line luminosity of HPQ (open squares) and BLL (filled squares and circles) appear similar. Upper limits flux (indicated by arrows) are computed assuming an e.w.=1Å for the maximum possible strength of the undetected line. Data do not show any evident segregation into two distinct populations.

Table 4. Published luminosity of [OIII] (5007) line.

object	our	published	reference
0403 − 133	3150	2080	Jackson & Browne 1991
0403 − 133	3150	3500	Oke et al. 1984
0403 − 133	3150	590	Blumental 1982
0736 − 017	150	118	Jackson & Browne 1991
0736 − 017	150	220	Steiner 1981
1253 − 055	1070	2000	Steiner 1981
1253 − 055	1070	1700	Yee 1980
1921 − 29	676	536	Jackson & Browne 1991
2243 − 12	2400	2060	Oke et al. 1984

units in $10^{40} ergs^{-1}$

erage (and associated error) were reported. For 5 sources we found in the literature measurements of the of [OIII] (5007Å) line luminosity that can be directly compared with our values (see table 4). Although significant variations exists between different authors, a general agreement within a factor of 2 is found.

Due to the different redshift of the sources and the general weakness of lines we chose the H_β and MgII (2798 Å) lines for a comparison study of line properties of blazars and LPQ. These two lines are among the strongest observed in the optical band and are detected in a large fraction of the objects.

First of all we compare the line luminosities of blazars (HPQ+BLL) and LPQ. Fig. 8a reports the cumulative distribution of H_β luminosity for 12 blazars (17% of the sample, see table 3) with data by Yee (1980) for a 29 LPQ sample. The two distributions are different at the 95% confidence level. On average H_β is ∼6 times more luminous in LPQ than in blazars. The redshift distribution of our 12 blazars with detected Hβ and the one of the Yee sample are statistically indistinguishable. Moreover, quasars of the Yee sample are from a variety of catalogs (as 3C, PKS, etc.) that select sources in completely different ways. This ensure that no strong bias or evolutionary effects can be responsible of the observed difference.

Similar results are derived for the MgII line (28 values, 38%) compared with data reported by Oke, Shield & Corycanski (1984) for another sample of quasars distributed in a narrow redshift range ($0.5 < z < 0.7$). This sample includes 30 objects, 5 of which are HPQ. We therefore removed these sources (0403-133, 3c279, 1522+155, 1958-179, 2243-124) obtaining a sample of 25 LPQ with measured MgII luminosity. The cumulative distributions of MgII (Fig. 8b) are again different at 95% confidence level and also in this case blazars have weaker lines by a factor of ∼6. The Oke, Shield & Corycanski's sample includes quasars selected in many different ways with an average redshift of 0.60. This is smaller than the average redshift of our 28 blazar with detected MgII ($< z >= 0.90$). Due to the luminosity–distance correlation, on average our blazar should have more luminous lines than Oke, Shield & Corycanski's sources. Therefore the observed difference of 6 times in luminosity is a lower limits of the true value.

Present data put on a more firm statistical basis the previous suggestion by Moore & Stockman (1981) and by Angel &

Stockman (1980), who found that blazars tend to have weaker lines than LPQ. We obtained the same result considering only HPQ instead of HPQ and BLL together.

A major question about the blazar class is to understand if BLL and HPQ have different intrinsic emission lines luminosities. We investigate this point considering data for MgII (2798 Å) emission line (detected in 28 objects, tab 3) because in most BLL it is the stronger line and therefore the e.w.$<$ 5Å definition criteria apply just to this line. Since we only have MgII (2798 Å) data for a few BLL, we included the measurements of MgII luminosities reported by Stickel et al. (1993) for 6 radio selected BL Lac objects of the 1 Jy sample. Note that all available data are for radio selected sources, so we are forced to restrict the following consideration to RBL only. In our sample RBL and HPQ have the same redshift distribution; this remain true with the addition of the Stickel data. We therefore do not expect that significant different evolutionary effects can influence the following considerations. The luminosity of MgII (2798 Å) line versus redshift for HPQ and RBL is shown in Fig. 9. To make the comparison significant one has to consider that due to the difficulty to detect faint lines a correlation is induced between lines luminosity and redshift. To overcome this problem, one can analyze objects at the same z. We used two redshift intervals ($0.5 < z < 0.7$ and $0.85 < z < 1.05$) that contain 13 and 17 objects, respectively. Within these redshift bins the sources are uniformly distributed in the luminosity range of 10^{42} to 10^{44} erg/s. Although RBL preferentially have weaker lines, a large overlap of line luminosity between HPQ and RBL is present without indication of segregation into two distinct populations.

At this point, it is important to investigate the influence of the e.w.$<$5 Å definition criterium for BLL. As stated before, we classified our source following this prescription. As the e.w. depends on both continuum and line luminosity, some time a source with small e.w. line can still have a luminous line, provided the continuum is proportionally bright, but on average we expect to find that objects classified as BLL according to the above criterium have smaller line luminosity than HPQ. This is exactly what appear to be the case in Fig. 9. The effect of the definition criteria is even more evident plotting our blazars in the continuum–line luminosity plane (see Fig. 10).

It is found that the two quantities are well correlated and that, due to the definition criteria, all RBL lies in region corresponding to e.w.$<$5Å (but not 1308+326 which is inconsistently included in the 1Jy sample also if its MgII line has e.w = 37.2Å). Altogether, RBL fill the region of high continuum and low line luminosity, span nearly all values of line luminosity spanned by HPQ, while at a given line luminosity the continuum is higher than in HPQ making the e.w smaller. A continuum exist in line luminosity going from HPQ to BLL indicating that the 5Å limits is rather arbitrary. Just choosing as limit 10 or 1 Å for the e.w. we clearly change the classification of several sources.

The bias induced by the classification criteria can be roughly quantified assuming that the objects are uniformly distributed in the continuum flux and e.w. space. From Fig. 10 (or table 3) we can constrain the e.w. to vary between 0 and $\sim$ 80. Under this assumption, we expect BLL to have an average e.w. of 2.5,

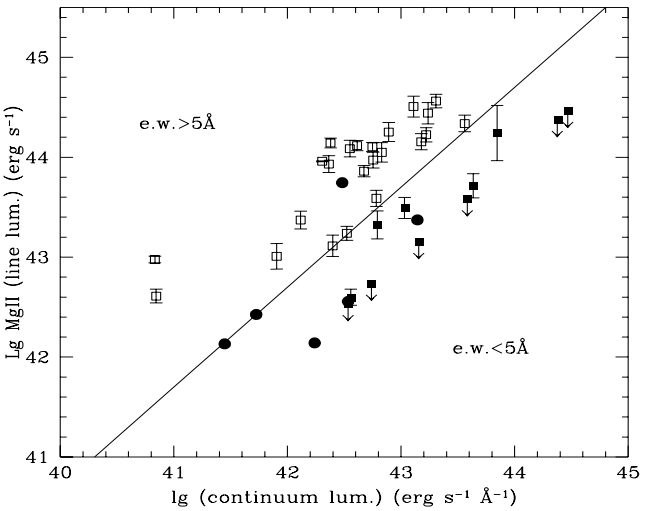

Fig. 10. The MgII 2798 Å line luminosity plotted versus the continuum luminosity below the line. As expected by the definition criteria, all BL Lac objects (filled squares = our data; filled circles = Stickel et al. 1993; upper limits correspond to e.w.=1 Å) lie in region with e.w.$<$5 Å indicated by the straight line. The BLL in the "wrong" region is 1308+326 which is not consistent with the standard definition as its MgII lines have e.w. rest frame of 18.6Å. Both HPQ (open square) and BLL show a correlation between the line and continuum luminosities, with BLL spanning similar line luminosity than HPQ but having higher continuum.

because the e.w. can range only between 0 and 5. On the other hand, HPQ should have an average e.w. of $(80 - 5)/2 \sim 38$. This translates into a factor of $\sim$ 15 in line flux. A bias of this order of magnitude easily explains the different line luminosities observed in the 1Jy sample of BLL and the 2Jy sample of flat spectrum radio quasar, which are basically all HPQ (Padovani 1992). Apart for the very small number of objects analyzed that makes the statistic quite unreliable, the mean luminosity of the [O III] 5007 emission line in the two samples differ by a factor of $\sim$ 100. Due to the luminosity–distance correlation, the different average redshift of the two samples (0.56 and 1.15,respectively for 1Jy and 2Jy sample) introduces a difference in line luminosity of $\sim (d_2/d_1)^2$ = 6.4, where d_1 and d_2 are the average luminosity distance of the two samples. We therefore expect a difference in line luminosity of $6.4 \times 15 \sim 100$, fully consistent with the reported result. We conclude that from the point of view of emission line properties HPQ and RBL are quite similar objects with the latter being simply the objects with (by definition) smaller e.w..

The luminosity of the MgII emission line does not show any significant dependence neither on the spectral index, nor on the amount of polarization (see Fig. 11).

4. Summary and conclusions

We discussed spectrophotometric optical observations for a sample of 73 blazars. The data, have been used to compare con-

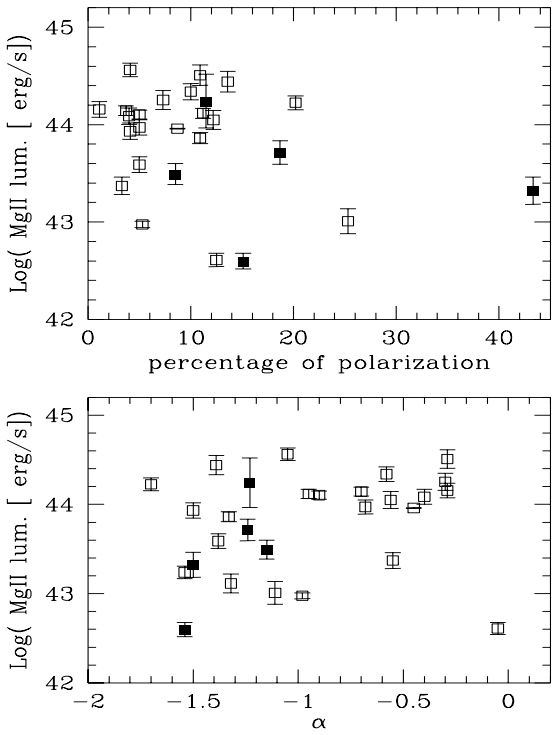

Fig. 11. MgII line luminosity versus maximum polarization (upper panel) and α_O (lower panel). No evident correlation is found in both cases. (Open square are HPQ, filled square are BLL).

tinuum and emission lines properties of HPQ, BLL, and LPQ. Our main conclusions are here summarized:

1. The optical spectral flux distribution of blazars, after removing the host galaxy component when relevant, is smoother and steeper than that of low polarization quasars. The overall radio-to-X-ray spectral index of HPQ and RBL is quite similar while XBL show systematically flatter continua. On the other hand the distribution of optical spectral indices α_O of HPQ suggests the presence of a population of flat optical spectrum objects.
2. Blazars show a significant correlations between the maximum optical polarization and both α_O and α_{RX}. The more polarized sources having the steepest spectra.
3. The study of H_β and MgII (2798 Å) line luminosities shows that blazars emission lines are ~ 6 times weaker than those of LPQ. The data put on a more solid statistical basis the suggestion by Moore & Stockman (1981) and by Angel & Stockman (1980).
4. The distributions of emission lines intensity for HPQ and BLL (but only data for RBL are available) are rather similar. BLL being, from the point of view of emission line properties, just the objects with same line luminosity of HPQ but with stronger continuum. The distribution of HPQ and BLL in the continuum-luminosity versus line-luminosity plane, shows that the alleged smaller line luminosity in BLL is biased by the selection criterium (e.w.$<$5Å) which preferentially includes in this class objects with weak lines. From this point of view it is not necessary to invoke two different populations of blazars (HPQ and BLL).

Actually, for a substantial fraction of BLL no emission line information is available. Many of them exhibits only some intervening absorption and/or absorption features from the host galaxy. For several sources the redshift remains unknown and no conclusions can be drawn for their intrinsic properties. Nevertheless the suggested strong connection between HPQ and RBL is extremely important since it influences the estimate of the luminosity function of both BLL and HPQ. This could force a revision of proposed unification schemes based on statistical counts. A major effort is clearly necessary to measure line intensity (or derive good upper limits) in no emission blazars and mainly in XBL. Present results make clear that objects have to be selected regardless their emission line properties otherwise results on emission lines them self will be meaningless.

Acknowledgements. The authors thank Guido De Marchi, C. Megan Urry, Joe Pesce, Aldo Treves, Elena Pian and the anonymous referee for helpful suggestions and comments to this manuscript. RS is grateful to the Visitor Program at STScI for hospitality and the ESO observatory for the good technical support at the telescope.

References

Angel J.R.P., & Stockman H.S. 1980, ARA&A, 18, 321
Ballard K. R., Mead A.R.G., & Brand P. W. J. L. 1990, MNRAS, 243, 640
Blandford R. D. & Rees M. J. 1978, in Pittsburgh Conference on BL Lac Objects, ed. A. N. Wolfe (Pittsburgh, University of Pittsburgh Press), p. 328
Blumenthal G.R., Keel W. C. & Miller J. S. 1982, ApJ 257, 499
Brindle C., Hough J. H., Bailey J. A., Axon D. J., & Hyland A. R. 1986, MNRAS 221, 739
Brindle C., Hough J. H., Bailey J. A., Axon D. J., & Sparks W. B. 1991, MNRAS 252, 288
Brunner H., Lamer G., Worrall D. M., & Staubert R. 1994, A&A 287, 436
Cardelli J.A., Clayton G.C., & Mathis J.S. 1989, ApJ 345, 245
Elvis M., Lockman F. J., & Wilkes B.J. 1989, AJ 97, 777
Falomo R., Scarpa R., & Bersanelli M. 1994, ApJS 93, 125 (FSB94)
Francis P.J. 1996, PASA 13, 212
Fugmann W. 1989, A&A 205, 86
Fugmann W., & Meisenheimer K. 1988, A&AS 76, 145
Ghisellini G., Maraschi L., Tanzi E. G., & Treves A. 1986, ApJ 310, 317
Giommi P., Ansari S. G., & Micol A. 1995, A&AS 109, 267
Impey C.D., & Neugebauer G. 1988, AJ 95, 307
Impey C.D., & Tapia S. 1988, ApJ 333, 666
Impey C.D., & Tapia S. 1990, ApJ 354, 124
Impey C.D., Lawrence C. R., & Tapia S. 1991, ApJ 375, 461
Jackson N. & Browne I. W. A. 1991, MNRAS 250, 414
Jannuzi B. T., Smith P. S., & Elston R. 1994, ApJ 428, 130
Kinman T. D. 1976, ApJ 205, 1
Kollgaard R. I., Wardle J. F. C., Roberts D. H., & Gabuzda D. C. 1992, AJ 104, 1687
Kollgaard R. J. 1994, Vistas Astron. 38, 29
Kühr H. & Schmidt G. D. 1990 AJ 99, 1
Landau R. et al. 1986, ApJ 308, 78

Ledden J.E., & O'Dell S.L. 1985, ApJ 298, 630
Mead A.R.G., et al. 1990, A&AS 83, 183
Miller J.S., French H.B., & Hawley S.A. 1978, in Pittsburgh conference on BL Lac objects, ed. A.M. Wolfe (University of Pittsburgh Press), p 176
Moore R.L., & Stockman H.S. 1981, ApJ 243, 60
Moore R.L., & Stockman H.S. 1984, ApJ 279, 465
Nass, P., Bade, N., Kollgaard, R. I., Laurent-Muehleisen, S. A., Reimers, D. & Voges, W. 1996, A&A 309, 419
Oke J. B., Neugebauer G., & Becklin E. E. 1969, ApJ 156, L41
Oke J. B., Shield G. A., & Corycanski D. G. 1984, ApJ 277, 64
Padovani P. 1992, MNRAS 257, 404
Padovani P., Giommi P., & Fiore F. 1997, MNRAS 284, 569
Pian E., Falomo R., Scarpa R., & Treves A. 1994, ApJ 432, 574
Rieke G.H., Lebofsky M., & Kinman T. D. 1979, ApJ 232, L151
Rieke G.H., & Lebofsky M. 1985, ApJ 288, 618
Sambruna R. 1997, in preparation
Sambruna R. 1995, Doctor thesis
Scarpa R., Falomo R., & Pian E. 1995, A&A 303, 730
Shull J.M., & Van Steenberg M.E. 1985, ApJ 294, 599
Smith P. S., Balonek T. J., Elston R., & Heckert P. A. 1987, ApJS 64, 459
Stark A. A., Gammie C. F., Wilson R. W., Bally J., Linke R. A., Heiles C., Hurwitz M., 1992, ApJS 79, 77
Steiner J.E. 1981, ApJ 250, 469
Stickel M., Padovani P., Urry C.M., Fried J.W., & Kuhr H. 1991, ApJ 374, 431
Stickel M., Fried J.W., & Kuhr H. 1993, A&AS 98, 393
Stockman H. S. & Angel J. R. P. 1978, ApJ 220, L67
Stone R.P.S. 1977, ApJ 218, 767
Ulrich M. H. 1981, A&A 103, L1
Urry C. M. & Padovani P. 1995, PASP 107, 803
Valtaoja E., Teräsranta H., Urpo S., Nesterov N. S., Lainela M., & Valtonen M. 1992, A&A 254, 80
Vermeulen et al. 1995, ApJ 452, L5
Véron-Cetty M. P. & Véron P. 1993, A catalogue of Quasars and Active Galactic Nuclei, ESO Scientific Report No. 13
von Montigny C. et al. 1995, ApJ 440, 525
Wills B. J. et al. 1983, ApJ 274, 62
Wills B. J., Wills B. J., Breger M., & Hsu J. C. 1980, AJ 85, 1555
Wills B. J. 1986, on Quasars; Proceedings of the IAU Symposium, Bangalore India. Dordrecht, D. Reidel Publishing Co., p.279
Wills B.J., Wills D., Breger M., Antonucci R. R. J., & Barvainis R. 1992, ApJ 398, 454
Worrall D. M. & Wilkes B. J. 1990, ApJ 360, 396
Yee H. K. C., & Oke J. B. 1978, ApJ 226, 753
Yee H. K. C. 1980, ApJ 241, 894

This article was processed by the author using Springer-Verlag LaTeX A&A style file *L-AA* version 3.